Indian Journal of Engineering & Materials Sciences
Vol. 10, February 2003, pp. 82-86

Spectro-structural and microscopic studies on solution-grown $CdS_{1-x}Te_x$ thin films

V B Patil[a*], G S Shahane[b] & L P Deshmukh[a]

[a]Department of Physics, Shivaji University Centre for P.G. Studies, Solapur 413 002, India

[b]Department of Electronics, DBF Dayanand College of Arts and Science, Solapur 413 002, India

Received 8 April 2002; accepted 13 August 2002

Compositional, structural, microstructural and optical properties of thin films of $CdS_{1-x}Te_x$ ($0 \leq x \leq 1$) prepared by the solution-growth technique are reported as a function of x. The film composition has been determined and compared with the bath composition. A non-linear relation has been found between them. The composites are crystalline in nature and pure CdS and CdTe existed in both hexagonal wurtzite and cubic zinc blende structures. Only wurtzite structure undergoes solid solution in the region $0 \leq x \leq 0.1$ and $0.9 \leq x \leq 1$. For $0.1 < x < 0.9$ the films have been composed of the mixed phases of CdS and CdTe. The lattice parameters a and c vary with x following Vegard's law in the solid solution region. The surface topography showed polycrystalline texture with a rough surface and diffused grain structure. Optical studies revealed a high absorption coefficient (10^4-10^5 cm^{-1}) with direct type of transition.

Solid solution formation in semiconductors is of great interest because of it results in new semiconductor series, thus broadening the scope of possible technological advances. The II-VI compounds are of great importance in this respect since band gaps in these series can be tailored to encompass the wavelengths of relevance to both light (solar) to electrical energy conversion and detectors for optical communications[1-3]. Attempts were therefore made in this study to prepare thin solid solution films of the type $CdS_{1-x}Te_x$ by employing an inexpensive solution growth technique[4-8] and reported on some of the film properties with special emphasis given to the film composition, crystal structure, microstructure and optical properties of the film.

Experimental Procedure

$CdS_{1-x}Te_x$ thin films were grown onto micro glass slides, which were first cleaned in chromic acid, followed by repeated washing in boiling deionized water. Once cleaned, the slides were mounted vertically in a beaker containing a deposition mixture maintained at a temperature of 75°C. The deposition mixture contained five solutions (freshly prepared from deionized water): (i) 1 M cadmium sulphate, (ii) 1 M thiourea, (iii) 7.5 M triethanolamine, (iv) 14 N ammonia and (v) sodium tellurosulphite, obtained by refluxing tellurium powder with anhydrous sodium sulphite in water, was added slowly to the reaction mixture by a separate arrangement. All the chemicals used were of AR-grade purity. The above solutions were mixed by varying the relative proportion of thiourea and sodium tellurosulphite solutions and taking cadmium sulphate in a particular ratio to get a starting solution having a different thiourea-to-tellurium mole percentage ratio. Thus, $CdS_{1-x}Te_x$ films with various compositions x (Te-concentration) varying from 0 to 1 can be deposited. The beaker containing the slides and the deposition mixture was vigorously stirred magnetically during deposition. After 90 min, the slides were removed and washed with deionized water to remove loosely bound $CdS_{1-x}Te_x$ powder and finally cleaned ultrasonically. In some instances, multilayers of $CdS_{1-x}Te_x$ films were deposited by repeating the above process.

The composition of the films was determined by EDS (KEVEX: 7000–77). The crystal structure of the films was determined by XRD using CuKα radiation, $\lambda = 1.5418$ Å (Philips PW-1710) for $2\theta = 10$ to 80°C. The microstructural properties were studied by SEM (CAMECA SU-30, France). A spectrophotometer, Hitachi-330, was used to record the optical absorbance of the sample in the 350-950 nm wavelength range. The absorption coefficient (α), optical gap (E_g) and the type of transition were determined from these studies.

*For correspondence

Results and Discussion

Specular and adhesive thin films of $CdS_{1-x}Te_x$ grown by the solution growth technique were obtained throughout the composition range ($0 \leq x \leq 1$). As-grown $CdS_{1-x}Te_x$ films are bright yellow oranges and the yellowness increases with increasing tellurium concentration. Pure CdTe films are white gray in colour[9].

Compositional analysis

Composition of the CdS_{1-x} Te_x films in the whole range was determined by EDS analysiss and it is evident that the films are nearly stoichiometric. Different parts of the films were checked for compositional analysis and a slight variation in the composition was found which shows that the films are nearly homogeneous and is shown in Fig. 1.

Crystal structural properties

In the composition range $0 \leq x \leq 1$, the crystal structure of the $CdS_{1-x}Te_x$ films has been determined from X-ray diffraction technique within the scanning range from 10-80 ° (Fig. 2). It is seen that all the samples are crystalline over the whole range studied. From the ASTM data it is seen that pure CdS has the strongest diffraction peak corresponding to (101) reflection for the hexagonal phase and (111) reflection for the cubic phase. From our experimental observations, pure CdS has the strongest diffraction peak at the interplaner distance d = 3.101 Å, which can be indexed as (101) plane of the hexagonal phase[10]. Other major peaks of the hexagonal (d = 3.353 Å and d =1.767 Å) reflection and the cubic (d = 2.90 Å and d = 2.058 Å) reflections are also present indicating that pure CdS exists in both hexagonal wurtzite and cubic zinc blende structures. Addition of tellurium

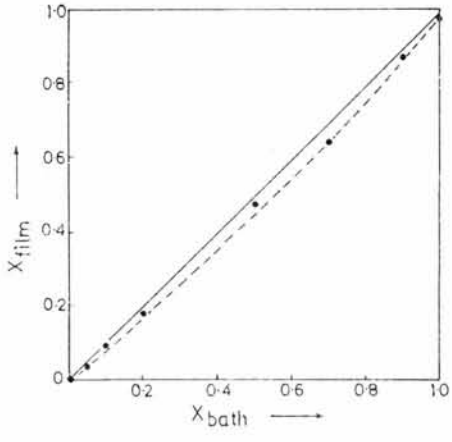

Fig. 1—Variation of x_{film} with x_{bath}.

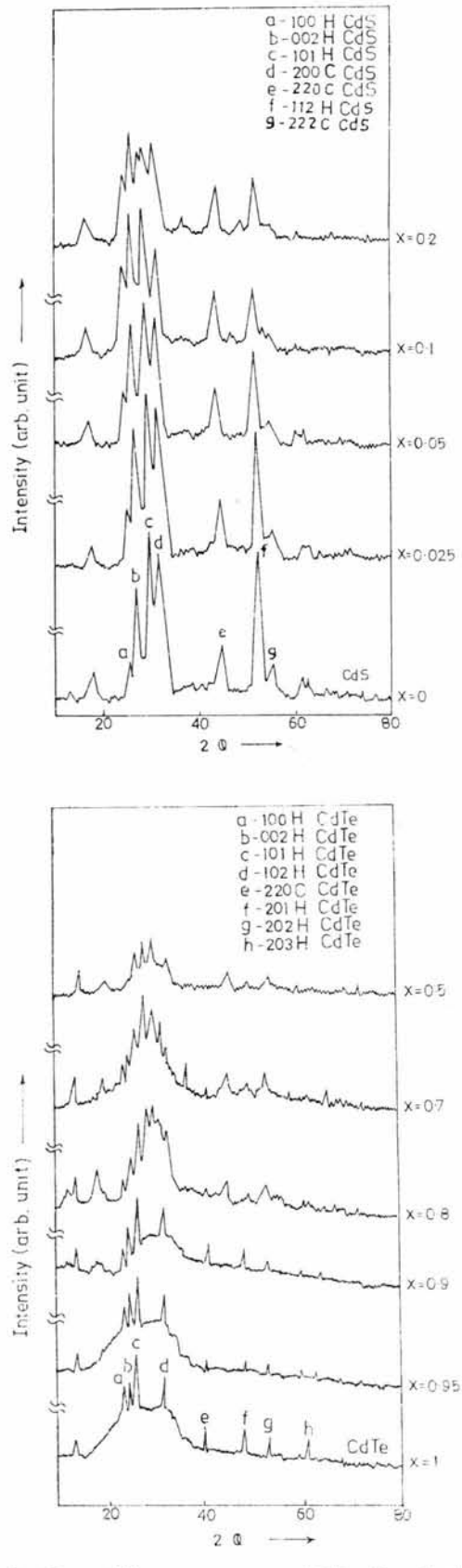

Fig. 2—X-ray diffractogram traces of $CdS_{1-x}Te_x$ thin films.

into the lattice of CdS shifts the peak position of the hexagonal phase towards lower 2θ side. This shift is continuous up to $x = 0.1$, indicating the formation of solid solution in the range $0 \le x \le 0.1$. Thereafter, the positions of these peaks remained more or less the same up to $x = 0.9$. In addition, for $x \ge 0.15$, few reflections of CdTe (hexagonal and cubic) are detected. Thus for higher values of x (≥ 0.15) formation of separate phases of both CdS and CdTe took place. For still higher values of x ($0.9 \le x \le 1$) the behaviour is again interesting. Only the peaks of CdTe (hexagonal and cubic) are detected, hexagonal being dominant. The most intense peak has been found to be shifted continuously reaching finally $d = 3.330$ Å which is (101) reflection of hexagonal CdTe[11]. This has clearly indicated the formation of solid solution in this range also. Few reflections of cubic CdS and CdTe remained more or less at the same position. This clearly showed that cubic phase remained unaltered and does not contribute to the formation of solid solution. The lattice parameters have been determined for all the compositions. Fig. 3 shows the variation of lattice parameters of the hexagonal phase with composition in the solid solution range. The variation is almost linear and obeys Vegard's law. The average grain size of the crystallites can be determined by using well-known Scherrer's relation[12];

$$D = \frac{k\lambda}{B\cos\theta} \qquad \ldots (1)$$

where k is constant related to the shape of the crystallites and indices of the reflecting planes. The average crystallite size has been determined for all the compositions and is given in Table 1.

Microstructural properties

Scanning electron micrographs of as-deposited

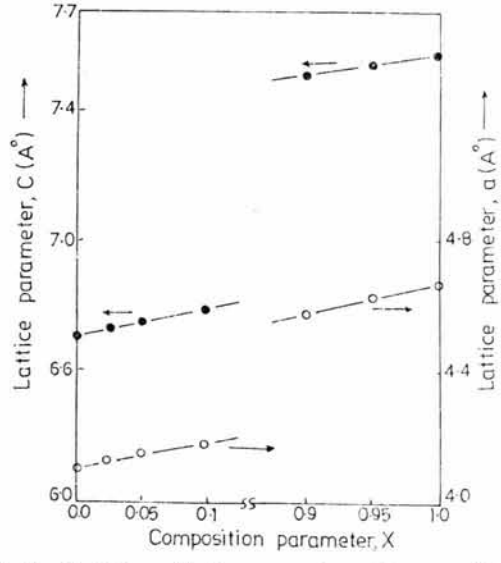

Fig. 3—Variation of lattice parameter with composition parameter, x

Table 1—Composition dependent properties of $CdS_{1-x}Te_x$ thin films

Composition x	Thickness t μm	Lattice parameters CdS (H) c, Å	CdS (H) a, Å	CdS (C) a, Å	CdTe (H) c, Å	CdTe (H) a, Å	CdTe (C) a, Å	Grain size D, Å	Band gap E_g, eV	Power factor n
0	0.79	6.700	4.101	5.813	—	—	—	127	2.42	1.02
0.025	0.78	6.724	4.120	5.828	—	—	—	136	2.39	0.88
0.05	0.73	6.742	4.143	5.840	—	—	—	149	2.36	0.80
0.075	0.72	6.751	4.154	5.842	—	—	—	170	2.34	0.92
0.1	0.67	6.762	4.163	5.844	—	—	—	222	2.31	0.96
0.15	0.65	6.714	4.123	5.818	7.498	4.618	6.490	167	2.27	1.20
0.2	0.66	6.708	4.118	5.824	7.501	4.602	6.490	146	2.21	0.88
0.3	0.55	6.698	4.113	5.812	7.513	4.590	6.476	143	2.13	0.86
0.4	0.53	6.692	4.129	5.807	7.510	4.610	6.480	144	2.03	1.04
0.5	0.48	6.692	4.129	5.807	7.508	4.580	6.470	156	1.94	0.84
0.6	0.44	6.690	4.116	5.815	7.500	4.580	6.470	170	1.84	1.12
0.7	0.45	6.692	4.127	5.815	7.512	4.600	6.476	164	1.74	0.88
0.8	0.41	6.692	4.125	5.815	7.510	4.580	6.478	168	1.64	0.96
0.9	0.39	—	—	—	7.500	4.580	6.462	198	1.53	0.98
0.95	0.36	—	—	—	7.524	4.562	6.482	204	1.50	0.96
1	0.32	—	—	—	7.542	4.650	6.484	210	1.46	1.04

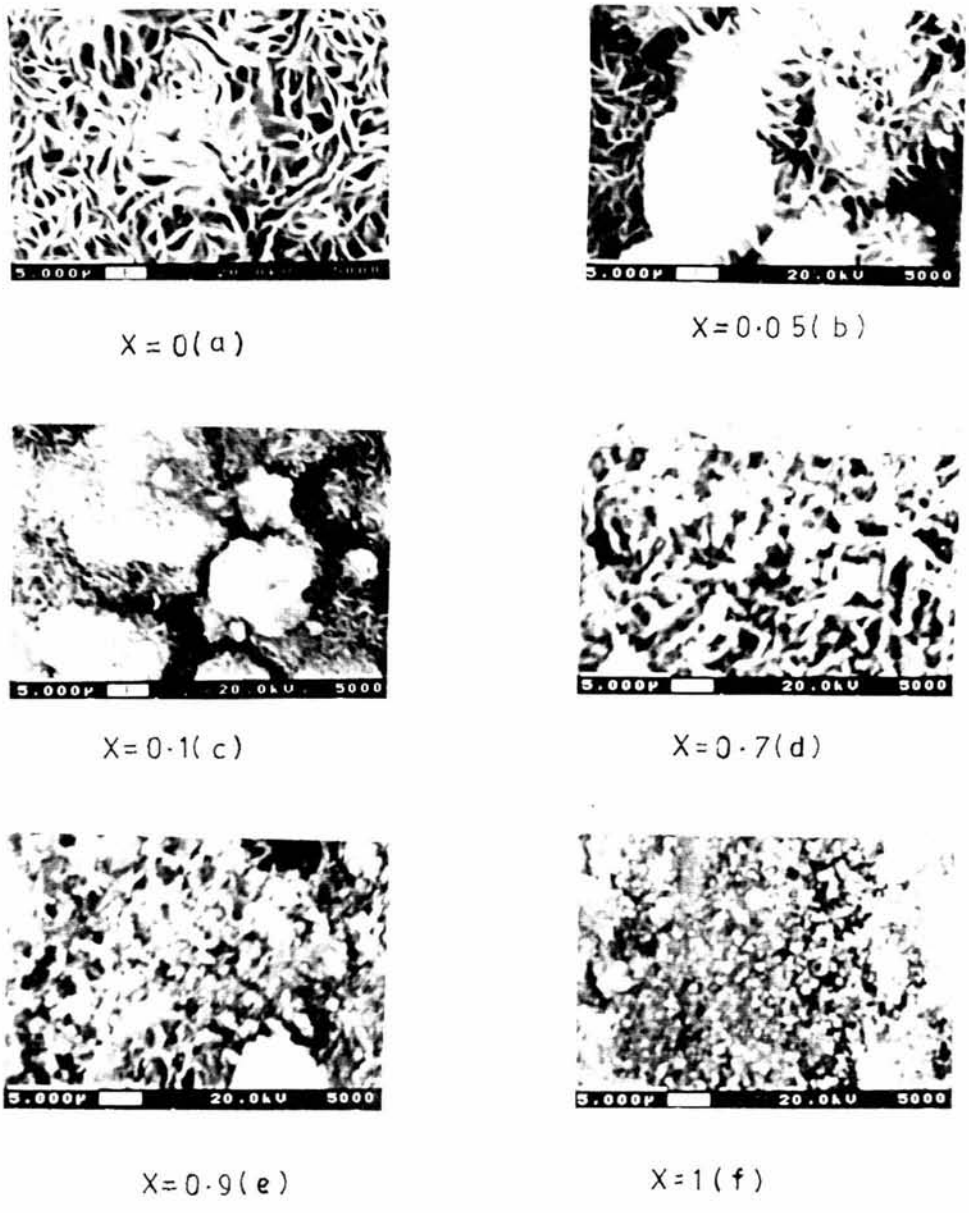

Fig. 4—SEM micrographs of six $CdS_{1-x}Te_x$ thin films with various x–values (on glass substrates).

$CdS_{1-x}Te_x$ films are shown in Fig. 4. It is evident from the micrographs, pure CdS appears like a mesh structure Fig. 4a. The results are similar to the observations of Bhushan and Shrivastava[13]. Padam *et al.*[14] called such appearance as fibrous structure. Results of Ma and Bube[15] have also supported these observations. For smaller values of x, the grain structure is found to be improved with increase in composition parameter (Figs 4b and 4c). The grains are found to be more closely packed and a considerable grain swelling is observed at $x = 0.1$ (Fig. 4c). For higher values of x, grain structure is disturbed and seems to be altogether different with reduced grain size. The surface morphology of CdTe showed a presence of small spherical and well-connected grains with a larger intergranular spacing[9]. The results are similar to the observations of Gore *et al.*[16] and Pal *et al.*[17] (Fig. 4f).

Optical properties

The optical absorption spectra of these samples were obtained and studied to evaluate the absorption coefficient (α), optical gap (E_g) and nature of the transitions involved. It is found that the optical absorption coefficient is higher for all the compositions (10^4 cm^{-1}) with a shift in the absorption edge from wavelength 520 nm to 860 nm as x was increased from

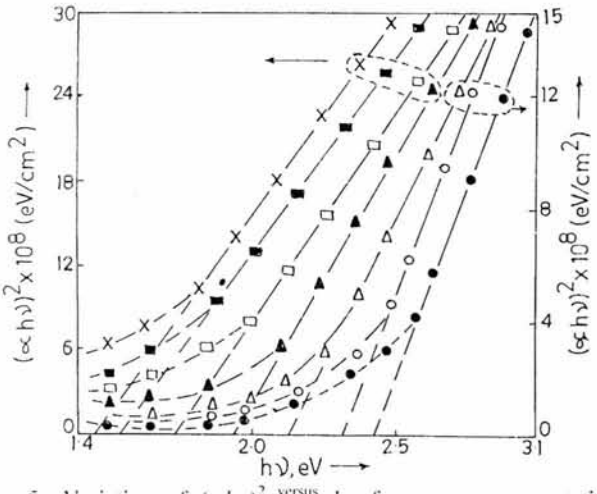

Fig. 5—Variation of $(\alpha h\nu)^2$ versus $h\nu$ for seven representative $CdS_{1-x}Te_x$ samples [x=0 (•), x=0.1 (○), x=0.3 (Δ), x=0.5 (▲), x=0.7 (□), x=0.9 (■) and x=1 (*)]

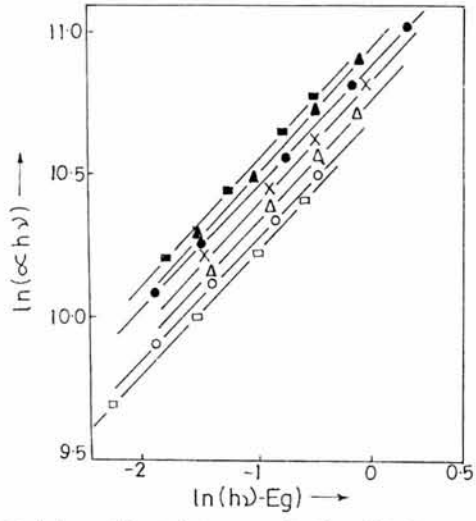

Fig. 6—Variation of ln ($\alpha h\nu$) versus ln ($h\nu - E_g$) for seven representative $CdS_{1-x}Te_x$ samples [x=0 (•), x=0.1 (○), x=0.3 (▲), x=0.5 (Δ), x=0.7 (■), x=0.9 (□) and x=1 (*)]

0 to 1. The absorption coefficient (α), energy gap (E_g), and the photon energy ($h\nu$) are related as[18,19]:

$$\alpha h\nu = A(h\nu - E_g)^{n/2} \quad \ldots (2)$$

Assuming the mode of transition to be of the direct allowed type (n = 1), the band gap energies have been computed from the variation of $(\alpha h\nu)^2$ versus $h\nu$ (Fig. 5). It is clear from the figure that the band gap is decreased typically from 2.42 eV to 1.46 eV as x is changed from 0 to 1. The mode of optical transition in these composite structure has been confirmed from the variation of $\ln(\alpha h\nu)$ versus $\ln(h\nu - E_g)$ (Fig. 6) which showed n nearly equal to 1 indicating the direct type of transition.

Conclusions

It is pointed out that the compositional, structural, microscopic and optical characteristic features observed for chemical bath synthesized $CdS_{1-x}Te_x$ thin films have close agreement with what had been observed for other semiconductor solid solution systems, which show their common characters. It is also shown that the alterations in the deposition history and chemical constituents in the Cd(S,Te) system lead to the composition scenarios ranging from a physical admixture of CdS and CdTe to a $CdS_{1-x}Te_x$ solid solution and even the superstructures with approximately alternating stacks of CdS and CdTe layers can be built. These characteristics make the solution growth process a simple and in expensive and attractive means of obtaining Cd(S,Te) thin films for a variety of applications.

Acknowledgements

The authors are grateful to Head, Regional Sophisticated Instruments Centre, Indian Institute of Technology, Mumbai for providing SEM and EDS facilities.

References

1 Hodes G, *Nature, (London)* 285 (1980) 29.
2 Russak M A & Creater C, *J Electrochem Soc*, 131 (1984) 556.
3 Gutierrez M T, *Solar Energy Mater*, 21 (1991) 283.
4 Chopra K L & Das S R, *Thin film solar cells* (Plenum Press, New York), 1983, 1.
5 Tanaka S, Mikami Y, Deguchi H & Kobyyashi H, *Jpn J Appl Phys*, 25 (1986) 225.
6 Suryanarayana C V, Laxshmanan A S, Subramanian V & Kumar R K, *Bull Electrochem*, 2 (1986) 57.
7 Deshmukh L P, More B M & Holikatti S G, *Bull Mater Sci*, 17 (1994) 455.
8 Gordillo G, *Solar Energy Mater Solar Cells*, 25 (1992) 42.
9 Patil V B, More P D, Sutrave D S, Mulik R N, Shahane G S & Deshmukh L P, *Mater Chem Phys*, 65 (2000) 282.
10 *ASTM card for X-ray diffraction data*, No. 6 – 0314 & 10-454.
11 *ASTM card for X-ray diffraction data*, No. 15 – 770 & 19-193.
12 Cullity B D, *Elements of X-ray diffraction* (Addison Wesley, Inc, New York), 1978, 102.
13 Bhushan S & Shrivastava S, *Indian J Pure Appl Phys*, 33 (1995) 371.
14 Padam G K, Malhotra G L & Rao S U M, *J Appl Phys*, 63 (1988) 770.
15 Ma Y Y & Bube R H, *J Electrochem Soc*, 124 (1977) 1430.
16 Gore R B, Pandey R K & Kulkarni S K, *Solar Energy Mater*, 18 (1989) 159.
17 Chakrabarti R, Ghosh S, Chaudhuri S & Pal A K, *J Phys D: Appl Phys*, 32 (1999) 1258.
18 Gerischer H, in *Semiconductor—Liquid Junction Solar Cells*, edited by Heller A (The Electrochem Soc Inc, Princeton, NJ), 1977, 1.
19 Chandra S & Pandya R K, *Phys Status Solidi (a)*, 92 (1982) 415.